HHS Public Access

Author manuscript

Nat Immunol. Author manuscript; available in PMC 2016 February 01.

Published in final edited form as:

Nat Immunol. 2015 August ; 16(8): 829–837. doi:10.1038/ni.3225.

The transcription factor XBP1 is selectively required for eosinophil differentiation

Sarah E. Bettigole[1,2,3], **Raphael Lis**[4,5], **Stanley Adoro**[2,3], **Ann-Hwee Lee**[6], **Lisa A. Spencer**[7], **Peter F. Weller**[7], and **Laurie H. Glimcher**[2,3]

[1]Program in Immunology, Harvard Medical School, Boston, MA

[2]Department of Medicine, Weill Cornell Medical College, Cornell University, New York, NY

[3]Sandra and Edward Meyer Cancer Center, Weill Cornell Medical College, New York, NY

[4]Ansary Stem Cell Institute, Department of Genetic Medicine, and Howard Hughes Medical Institute, Weill Cornell Medical College, New York, New York 10065, USA

[5]Ronald O. Perelman and Claudia Cohen Center for Reproductive Medicine, Weill Cornell Medical College, New York, New York 10065, USA

[6]Department of Pathology and Laboratory Medicine, Weill Cornell Medical College, Cornell University, New York, NY

[7]Division of Allergy and Inflammation, Department of Medicine, Beth Israel Deaconess Medical Center, Harvard Medical School, Boston, MA

Abstract

The transcription factor XBP1 has been linked to the development of highly secretory tissues such as plasma cells and Paneth cells, yet its function in granulocyte maturation has remained unknown. Here we discovered an unexpectedly selective and absolute requirement for XBP1 in eosinophil differentiation without an effect on the survival of basophils or neutrophils. Progenitors of myeloid cells and eosinophils selectively activated the endoribonuclease IRE1α and spliced *Xbp1* mRNA without inducing parallel endoplasmic reticulum (ER) stress signaling pathways. Without XBP1, nascent eosinophils exhibited massive defects in the post-translational maturation of key granule proteins required for survival, and these unresolvable structural defects fed back to suppress critical aspects of the transcriptional developmental program. Hence, we present

Correspondence should be addressed to: Laurie H. Glimcher, M.D., Weill Cornell Medical College, 1300 York Avenue, F-113, New York, NY 10065, USA, Tel: 212-746-6005, Fax: 212-746-8424, lglimche@med.cornell.edu.

Accession codes. GEO: Illumina RNA-seq raw sequence reads and read counts, GSE65753. Referenced gene expression analysis accession GEO: GSE55386

AUTHOR CONTRIBUTIONS

S.E.B. and L.H.G. designed and analyzed the experiments; S.E.B. conducted experiments and wrote the manuscript; R.L. performed high-resolution immunofluorescence microscopy imaging. S.A. contributed to the design of certain experiments; A.H.L. provided reagents, L.H.G., L.A.S., and P.F.W. supervised the research and edited the manuscript.

COMPETING FINANCIAL INTERESTS

The authors declare competing financial interests. L.H.G. is on the Board of Directors and holds equity in Bristol Myers Squibb Pharmaceutical Company.

evidence that granulocyte subsets can be distinguished by their differential reliance on secretory-pathway homeostasis.

Introduction

The endoplasmic reticulum (ER) is a critical regulator of calcium storage and signaling, lipid biosynthesis, and the proper folding and post-translational modification of secreted and transmembrane proteins. This organelle functions in a highly integrated manner to support these fundamental and interconnected biological processes, and disruptions in specific ER tasks are often counterbalanced by compensatory modulation of parallel ER abilities. ER dysfunction, or stress, can be caused by the intraluminal accumulation of misfolded proteins. If the influx of new protein substrates into the ER overwhelms its steady-state protein-folding capacity, a multi-pronged response known as the 'unfolded protein response' (UPR) is triggered to ameliorate cellular ER stress.

The UPR is driven by the combined action of the ER membrane–localized kinase-endoribonuclease IRE1α (encoded by *Ern1*), the transcription factor ATF6 and the kinase PERK. When ER stress occurs, IRE1α splices out 26 nucleotides from cytoplasmic *Xbp1* mRNA and thereby induces a shift in the reading frame that leads to the translation of a highly active transcription factor involved in the UPR[1]. PERK induces translational repression by phosphorylating the translation-initiation factor eIF2α[2], which subsequently activates the transcription factors ATF4 and CHOP (encoded by *Ddit3*)[3]. Simultaneously, ATF6, together with XBP1, regulates various genes encoding stress-response factors[4, 5]. This tripartite response reduces ER stress by upregulating the expression of genes encoding protein chaperones, redox enzymes and glycosylases to enhance protein folding within the ER while simultaneously reducing the overall translation rate to slow the influx of new proteins. Successful resolution of ER stress results in cellular adaptation and protection from future proteotoxic insults, while failure to ameliorate the offending stimulus leads to cell death.

XBP1 is best known as a major developmental regulator of highly secretory cells such as plasma cells[6], Paneth cells[7] and pancreatic acinar cells[8]. These cell types are generally equipped with extensive ER networks to cope with the burden of constitutive synthesis of secreted proteins upon terminal maturation. In the absence of *Xbp1*, a condition that can sensitize cells to ER stress by diminishing adaptive protein-folding capacity, such highly secretory cells generally demonstrate a disorganized ultrastructure of the endomembrane pathway and increased cell death[8]. Notably, XBP1 also supports the differentiation and survival of certain cell types that are not thought to engage in constitutively abundant production of secreted proteins, such as resting splenic dendritic cells[9]. We therefore postulated that developmental and cell-survival requirements for the UPR, and XBP1 in particular, might extend beyond 'professional' secretory cells due to the need to cope with transient but intense bursts of protein production encountered during development. To this end, we chose to study granulocyte differentiation as a model system for investigating the physiological importance of the UPR during intense, developmentally restricted demands on the secretory pathway.

Neutrophils, eosinophils and basophils constitute the three main types of granulocytes. Large quantities of neutrophils are produced and stored in the bone marrow, poised for rapid deployment to sites of infection and injury to destroy invading microorganisms and help coordinate type 1 immune responses[10]. In contrast, the comparatively rare eosinophils[11] and basophils[12] are typically associated with type 2 immune responses, allergy and parasitic infection. However, published reports have shown that these 'enigmatic' cells, particularly eosinophils, can serve important roles in the regulation of insulin sensitivity[13], adipose tissue development[14], regenerative responses to injury[15], tumor burden[16] and the survival of memory plasma cells[17].

The earliest stages of granulocyte differentiation are morphologically similar across lineages and are marked by rapid upregulation and intense production of granulocyte-specific effector proteins[18]. As differentiation progresses over several days, granule-protein production is gradually extinguished and components of the secretory pathway, including the ER, are substantially downsized[18]. Thus, granulocyte differentiation represents a tractable model system for investigating how the UPR, and XBP1 in particular, regulates survival and adaptation during physiologically relevant, temporally restricted states requiring high secretory-pathway functionality.

Here we report a highly selective and indispensable role for XBP1 and its upstream activator IRE1α in the development of mouse eosinophils but not of other granulocyte lineages. Hematopoietic ablation of *Xbp1* resulted in complete, cell-intrinsic loss of mature eosinophils and progenitors of eosinophils without affecting upstream precursors. Unbiased transcriptome analyses of hematopoietic progenitor populations along the eosinophil developmental continuum revealed that diminished basal ER protein-folding capacity actively prevented terminal maturation after the commitment of progenitor cells to the eosinophil lineage, in part by downregulating expression of *Gata1*, which encodes the master eosinophil lineage–commitment factor GATA-1, and genes encoding indispensable granule proteins. Collectively our findings identify an unexpected interplay between cellular stress and a major lineage-determining transcription factor and indicate that the IRE1α-XBP1 signaling axis is a potential therapeutic target for eosinophil-mediated diseases.

Results

XBP1 is indispensable for eosinophil production

To investigate a possible role for XBP1 in granulocyte development, we crossed mice expressing Cre recombinase from the hematopoietic compartment–specific *Vav1* promoter (*Vav1*-Cre mice) to mice with loxP-flanked *Xbp1* alleles (*Xbp1*$^{f/f}$ mice) to generate *Xbp1*$^{f/f}$*Vav1*-Cre mice (called '*Xbp1*^{Vav1} mice' here) for targeted deletion of *Xbp1* in the hematopoietic compartment. Total bone marrow cellularity was unaffected by loss of *Xbp1* (Supplementary Fig. 1), and the frequency of splenic T cells, B cells, macrophages, neutrophils and basophils was essentially equivalent in *Xbp1*$^{f/f}$ and *Xbp1*^{Vav1} mice (Supplementary Fig. 2a–i), which indicated that *Xbp1* deficiency was generally well tolerated across the immune system. Similar to results in published reports[9], *Xbp1*^{Vav1} mice exhibited a reduction of approximately twofold in CD11c^{+} splenic dendritic cells relative to their abundance in *Xbp1*$^{f/f}$ mice (Supplementary Fig. 2j,k). Unexpectedly, we observed

highly selective and complete ablation of the eosinophil lineage in *Xbp1*^{Vav1} bone marrow, spleen and blood compared with the abundance of this lineage in *Xbp1*$^{f/f}$ bone marrow (Fig. 1a–c). Cre expression alone had no effect on the number of peripheral eosinophils (Supplementary Fig. 3). The persistence of neutrophils and basophils was not due to the escape and population expansion of rare *Xbp1*-sufficient progenitor cells, as sorted bone marrow granulocytes exhibited robust deletion of *Xbp1* (Supplementary Fig. 4a,b). Because *Xbp1* mRNA is directly spliced by IRE1α, we sought to determine whether *Ern1*$^{f/f}$*Vav1*-Cre (*Ern1*^{Vav1}) mice were similarly deficient in eosinophils. *Ern1*^{Vav1} mice were a full phenocopy of the *Xbp1*^{Vav1} mice (Fig. 1d,e), which indicated that physiological eosinophil differentiation in mice was wholly dependent on the spliced form of *Xbp1*.

Eosinophilopoiesis involves physiological ER stress

Since XBP1 was an absolute requirement for eosinophil development, we next sought to determine whether the IRE1α-XBP1 pathway is temporally regulated during eosinophil differentiation. Hematopoietic stem cells identified as lineage marker–negative (Lin$^-$) Sca-1$^+$ c-Kit$^+$ (LSK) cells progressively commit to the eosinophil lineage after passing through the stages of Lin$^-$Sca-1$^-$c-Kit$^+$CD34$^+$CD16/32$^-$ common myeloid progenitor (CMP), Lin$^-$Sca-1$^-$c-Kit$^+$CD34$^+$CD16/32$^+$ granulocyte-macrophage progenitor (GMP) and IL-5Rα$^+$Lin$^-$Sca-1$^-$ c-Kit^{dim}CD34$^+$ eosinophil progenitor (EoP)[19]. Immature eosinophils upregulate their expression of the sialoadhesin Siglec-F, while fully mature eosinophils additionally express the chemokine receptor CCR3 (ref. 20). We sorted cells along the eosinophil-differentiation spectrum and evaluated the ratio of full-length *Xbp1* mRNA to active, spliced *Xbp1* mRNA by quantitative PCR, after validating *Actb* as a suitably stable housekeeping reference gene across multiple cell lineages (data not shown). Notably, *Xbp1* mRNA was progressively spliced during differentiation, with the greatest activation in GMPs and EoPs (Fig. 2a–c). Splicing of *Xbp1* mRNA correlated with the induction of numerous downstream genes that are targets of XBP1, such as *P4hb*, *Edem1* and *Sec24d* (Fig. 2d). Upon final cellular maturation, protein-synthetic demands drop considerably, which probably explains why terminally differentiated eosinophils no longer spliced *Xbp1* mRNA. In contrast, *Ddit3* was not upregulated during eosinophil differentiation (Fig. 2d), which suggested that the PERK axis was not induced. We were unable to detect expression of PERK by immunoblot analysis in any cell type examined except CCR3$^+$ eosinophils (data not shown), which again suggested that this UPR signaling branch was minimally active during eosinophil differentiation. However, we were unable to rule out the possibility that small amounts of PERK are phosphorylated during eosinophil differentiation. Collectively these results suggested that developing eosinophils underwent a branch-specific UPR characterized by activation of IRE1α without activation of PERK. Similar cases of selective branch use have been observed in both macrophages and plasma cells, although why branch selectivity occurs, in a teleological sense, remains poorly understood[21,22].

XBP1 specifically supports eosinophil lineage survival

Given that *Xbp1* mRNA was maximally spliced in GMPs, we next sought to determine whether XBP1 was required for the differentiation and survival of GMPs. The frequency of bone marrow GMPs in *Xbp1*^{Vav1} mice was similar to that in *Xbp1*$^{f/f}$ mice (Fig. 2e,f), despite robust deletion of *Xbp1* (Supplementary Fig. 4c). Therefore, despite a high frequency of

Xbp1 mRNA splicing in GMPs, XBP1 did not substantially affect their differentiation and steady-state survival. In contrast, the EoP compartment was much smaller in *Xbp1*^{Vav} mice than in *Xbp1*$^{f/f}$ mice (Fig. 2g,h), which indicated that XBP1 was required at the earliest identifiable eosinophil-committed developmental stage. As the *in vivo* roles of XBP1 in cellular differentiation often correlate with defects in cell survival[8], we sought to determine whether *Xbp1*^{Vav1} EoPs exhibited signs of enhanced cell death. As expected, residual EoPs from *Xbp1*^{Vav1} mice demonstrated increased staining of active caspases (Fig. 2i), which indicated that XBP1 sustained the viability of EoPs.

To determine whether XBP1 was required for commitment to the eosinophil lineage, we bred the *Xbp1*$^{f/f}$ mice onto the *Epx*-Cre (eoCRE) strain[23] to generate '*Xbp1*eoCRE' mice. The eoCRE knock-in strain expresses Cre from the open reading frame of the endogenous gene encoding eosinophil peroxidase (*Epx*) and thus expresses Cre only after commitment to the eosinophil lineage and is exceedingly specific for eosinophils rather than cells of other hematopoietic lineages[23]. *Xbp1*eoCRE mice had a significantly smaller bone marrow eosinophil population than *Xbp1*$^{f/f}$ mice had (Fig. 2j,k) and, notably, the surviving peripheral eosinophils had escaped deletion of *Xbp1* (data not shown). Thus, XBP1 was needed to sustain viability of the eosinophil-committed progenitor.

Eosinophil development requires XBP1S cell-intrinsically

Eosinophil development relies on many transcription factors, such as GATA-1 and PU.1, but is also regulated by extracellular cues, such as interferon-γ[24]. To address whether the observed phenotype stemmed from cell-intrinsic or cell-extrinsic defects, we generated mixed–bone marrow chimeras by injecting a 1:1 mixture of congenically marked CD45.1^{+} wild-type cells and CD45.2^{+} *Xbp1*$^{f/f}$ or *Xbp1*^{Vav1} cells into lethally irradiated CD45.1^{+} recipient mice. We found that *Xbp1*^{Vav1} CD45.2^{+} cells were completely incapable of generating mature eosinophils, although their production of neutrophils and basophils was normal (Fig. 3a,b), which indicated that XBP1 functioned in a cell-intrinsic way to sustain eosinophil development. In further support of those findings, our efforts to generate *Xbp1*^{Vav1} bone marrow–derived eosinophils (BMDEs)[25] were unsuccessful, even in cultures containing interleukin 5 (IL-5) supplemented with additional pro-survival cytokines, such as IL-3 and GM-CSF (Fig. 3c and data not shown). The frequency of Siglec-F^{+} cells was significantly lower in *Xbp1*^{Vav1} cultures than in *Xbp1*$^{f/f}$ cultures at days 8 and 10 (Fig. 3d), when eosinophil populations are normally rapidly expanding. *Xbp1*^{Vav1} cells failed to acquire the characteristic eosinophil granule-associated high-side-scatter profile or to form proliferating colonies (Fig. 3c,e). Furthermore, cytospin analysis of Siglec-F^{+} BMDEs at day 8 that were negative for the DNA-binding dye DAPI (DAPI^{-}), which had been purified by flow cytometry, revealed that nascent eosinophils derived from *Xbp1*^{Vav1} cells initiated nuclear segmentation but were incapable of generating mature eosinophilic granules (Fig. 3f), indicative of arrested development. Notably, blocking IRE1α with the potent small-molecule inhibitor 4μ8C[26] had no effect on the survival of fully differentiated eosinophils from the bone marrow (had no effect on survival of fully differentiated eosinophils from the bone marrow (Supplementary Fig. 5). We noted similar effects on splenic eosinophils purified from mice with transgenic IL-5 expression[27] and in mature BMDEs incubated with concentrations of 4μ8C as high as 64 μM (data not shown). The function of XBP1, therefore,

mapped in a cell-intrinsic way to a developmental window after commitment to the eosinophil lineage but before terminal differentiation.

We next sought to determine whether ectopic overexpression of various *Xbp1* mRNA isoforms could 'rescue' the developmental defects in eosinophils. Retroviral overexpression of full-length, unspliced but spliceable *Xbp1* mRNA (*Xbp1us*) or its shorter, spliced isoform (*Xbp1s*) fully restored eosinophil development *in vitro* (Fig. 4a,b). However, *Xbp1*^{Vav1} cells were not 'rescued' by the over-expression of a full-length, unspliceable *Xbp1* mRNA variant (*Xbp1u*) (Fig. 4a,b), which further established the requirement for the *Xbp1s* isoform in eosinophilopoiesis. Of note, the 'rescued' cells displayed full morphological recovery (Fig. 4c). Thus, the substantial eosinophil developmental defects observed in *Xbp1*^{Vav1} mice could be readily corrected *in vitro* but only when the spliced *Xbp1s* RNA isoform was supplied.

Developmental networks are XBP1-independent in GMPs

Beyond its functions in maintaining ER homeostasis, XBP1 can control cell-type-specific transcriptional networks, including major cell-identity determinants, such as *Mist1* in myoblasts[28]. Therefore, we sought to determine whether XBP1 might influence the expression of known eosinophil developmental regulators in GMPs. GATA-1, GATA-2, C/EBPα, C/EBPβ, CEBPε, IRF8, PU.1, Id2 and TRIB1 positively regulate eosinophil development, while FOG1 and Id1 act as negative regulators[29,30]. Despite the presence of robust splicing of *Xbp1* mRNA, all known regulators of eosinophil development were expressed normally in *Xbp1*-deficient GMPs (Fig. 5a), which indicated that XBP1 was dispensable for the baseline expression of canonical regulators of eosinophil differentiation.

Attempts to isolate the few remaining CD34^{+} EoPs from *Xbp1*^{Vav1} mice were unsuccessful due to technical limitations (data not shown). Therefore, to delineate the effect of *Xbp1* deficiency after eosinophil commitment, we used a published strategy to enforce eosinophil differentiation on GMPs via retroviral overexpression of GATA-2 (ref. 31). Normally only ~1% of GMPs have the potential to develop into eosinophils, but overexpression of GATA-2 induces commitment to the eosinophil lineage[31]. We purified GMPs from *Xbp1*$^{f/f}$ and *Xbp1*^{Vav1} mice by flow cytometry and infected the cells with control retrovirus expressing green fluorescent protein (GFP) alone or retrovirus expressing GATA-2 and GFP; after 36 h, we re-sorted GFP^{+} (infected) cells and cultured the cells for various times[31]. While control retrovirus–transduced *Xbp1*$^{f/f}$ cells gave rise almost exclusively to macrophages and neutrophils, GATA-2-transduced cells demonstrated robust formation of eosinophilic granules and had high expression of genes encoding canonical markers of the eosinophil lineage (Supplementary Fig. 6a,b). However, similar to their maturation defects in BMDEs, secretory granules in GATA-2-transduced *Xbp1*^{Vav1} GMPs were immature compared with those in GATA-2-transduced *Xbp1*$^{f/f}$ GMPs (Supplementary Fig. 6c). Hence, GATA-2-transduced GMPs represented an effective phenocopy of critical aspects of eosinophil differentiation interrupted by loss of *Xbp1*.

After validating GATA-2 overexpression as a model for early eosinophil differentiation, we performed high-throughput sequencing for cDNA (RNA-seq) on freshly sorted GMPs and GATA-2- transduced GMPs from *Xbp1*$^{f/f}$ and *Xbp1*^{Vav1} mice to identify stage-specific,

XBP1-dependent processes. Of the 153 genes differentially expressed in *Xbp1*$^{f/f}$ GMPs versus *Xbp1*^{Vav1} GMPs, none encoded terminal eosinophil effectors (Fig. 5b and Supplementary Table 1), which suggested that defects in eosinophil development had yet to manifest. Additionally, pathway analysis identified alterations in canonical secretory pathway–associated processes, such as post-translational modifications, protein folding, carbohydrate metabolism, lipid metabolism, and organization of the Golgi apparatus (Fig. 5c and Supplementary Table 2). Despite the finding of reduced expression of genes encoding factors involved in multiple networks responsible for maintaining ER homeostasis, cellular viability and differentiation pathways were unaffected in GMPs, which indicated that deletion of *Xbp1* before commitment to the eosinophil lineage impaired the adaptive capacity of the ER without causing acute cellular impairment.

XBP1 sustains eosinophil development after commitment

Notably, in GATA-2-transduced GMPs cultured for 48 h, we observed pronounced downregulation of genes encoding several markers of terminal eosinophil differentiation (Fig. 6a and Supplementary Table 3). Genes encoding most known transcriptional regulators of eosinophil development generally had equivalent expression in GATA-2-transduced *Xbp1*$^{f/f}$ and *Xbp1*^{Vav1} GMPs, although the gene encoding GATA-1, a key transcription factor for eosinophil development, was modestly downregulated in GATA-2-transduced *Xbp1*$^{f/f}$ GMPs relative to its expression in GATA-2-transduced *Xbp1*^{Vav1} GMPs (Fig. 6b,c). Expression of the gene encoding GATA-2 was similar in *Xbp1*$^{f/f}$ and *Xbp1*^{Vav1} cells (Fig. 6c), which indicated that the effects on *Gata1* were not due to unequal ectopic overexpression of *Gata2*. Additionally, pathway analysis of potential upstream transcriptional regulators predicted that GATA-1 signaling was inhibited in *Xbp1*^{Vav1} cells, on the basis of downregulation of classic targets of GATA-1, such as *Cdkn2c*, *Abcb10* and *Prg2*, but only after commitment to the eosinophil lineage (Fig. 6d and Supplementary Table 2). Inefficient GATA-1-mediated signaling might have contributed to the loss of expression of genes encoding many eosinophil markers. Of the 200 genes differentially expressed in GATA-2-overexpressing *Xbp1*$^{f/f}$ GMPs versus their *Xbp1*^{Vav1} counterparts, less than 20% overlapped with genes known to be upregulated during BMDE differentiation[32], which indicated that loss of *Xbp1* inhibited limited and specific facets of the eosinophil developmental program.

We additionally observed that genes encoding products involved in amino-acid metabolism and cell-death pathways were markedly induced in GATA-2-transduced *Xbp1*^{Vav1} GMPs relative to their expression in GATA-2-transduced *Xbp1*$^{f/f}$ GMPs (Fig. 6e), which indicated that eosinophil differentiation without XBP1 was cytotoxic. The PERK signaling axis is considered to be pro-apoptotic and regulates amino-acid metabolism via ATF4 and CHOP[33], and we therefore sought to determine whether dysregulated gene expression reflected the activation of alternative UPR signaling branches. Consistent with that possibility, pathway analysis predicted ATF4 to be a strong mediator of the observed transcriptional changes (Fig. 6d). By quantitative PCR, we confirmed that the expression of several genes that are targets of ATF4 (*Ddit3*, *Asns* and *Trib3*) was upregulated in GATA-2-transduced *Xbp1*^{Vav1} GMPs compared with their expression in GATA-2-transduced *Xbp1*$^{f/f}$ GMPs (Fig. 6f). Unexpectedly, *Hspa5* expression was not higher in GATA-2-transduced *Xbp1*^{Vav1}GMPs

than in GATA-2-transduced *Xbp1*$^{f/f}$ GMPs (Fig. 6f), which suggested that *Xbp1* deficiency in eosinophil-committed cells activated an atypical, ATF4-dominated UPR.

The activation of PERK-ATF4 may have been driven by the accumulation of misfolded or incorrectly processed eosinophil-specific proteins. To investigate this possibility, we analyzed the posttranslational maturation of the eosinophil granule proteins PRG2 and EPX. Strikingly, we observed substantial accumulation of the 'pre-pro-forms' and/or 'pro-forms' of both granule proteins in *Xbp1*^{Vav1} cells after 96 h of culture (Fig. 7a–d), which indicated a nearly complete block in terminal post-translational maturation. Furthermore, ultrastructural analyses revealed substantial ER swelling and failure to nucleate granule packing (Fig. 7e), suggestive of ER stress and severe granule dysfunction upon commitment to the eosinophil lineage. Together these data suggested close coupling among ER homeostasis, eosinophil transcriptional identity, granule formation and cell death.

XBP1 links granulogenesis to *Gata1* expression

To verify the connection between XBP1 and the expression of granule proteins, we cultured BMDEs from *Xbp1*$^{f/f}$ and *Xbp1*^{Vav1} mice for 8 d, sorted DAPI^{-}Siglec-F^{+} cells and quantified expression of the gene encoding GATA-1 and genes encoding the key eosinophil effectors PRG2 and EPX. After 8 d of culture, *Xbp1*$^{f/f}$ BMDEs robustly express genes encoding key transcription factors as well as numerous genes encoding eosinophil markers[25]. All three genes (*Gata1*, *Prg2* and *Epx*) were markedly downregulated in *Xbp1*^{Vav1} BMDEs relative to their expression in *Xbp1*$^{f/f}$ BMDEs (Fig. 8a), which suggested that the expression of *Gata1* and terminal differentiation markers was 'titrated' by the 'health' of the secretory pathway. The transcriptional defects were more severe in Siglec-F^{+} BMDEs than in GATA-2-transduced GMPs (Fig. 8a), possibly because GATA-2 can upregulate *Gata1* expression[34]. Similarly, GATA-1 was essentially undetectable by immunoblot analysis in *Xbp1*^{Vav1} BMDE cultures at day 8 (Fig. 8b).

To further confirm that downregulation of *Gata1* occurred in eosinophil-committed cells, we performed immunofluorescence analysis of GATA-1 and PRG2 in *Xbp1*$^{f/f}$ and *Xbp1*^{Vav1} BMDE cultures. *Xbp1*$^{f/f}$ BMDEs co-expressed GATA-1 and PRG2, while the rare *Xbp1*^{Vav1} BMDEs, identified by granulocytic nuclear morphology and PRG2^{+} granules, completely lacked staining of GATA-1 (Fig. 8c). We were able to detect occasional GATA-1^{+} cells in *Xbp1*^{Vav1} BMDE cultures, but these cells never had eosinophil granules (Fig. 8d,e), which suggested that *Gata1* expression was mutually exclusive with granule formation under *Xbp1*-deficient conditions. To determine whether *Gata1* and genes encoding eosinophil granule proteins were direct targets of XBP1, we blocked XBP1 signaling for 8 h in developing BMDEs with 4μ8C. Unlike the expression of targets of XBP1 such as *Sec24d*, *Sec61a1*, *Dnajb9* and *P4hb*, the expression of *Gata1*, *Prg2* and *Epx* was unaffected by acute blockade of IRE1α (Fig. 8f), which indicated that these genes were not directly regulated by IRE1α-XBP1 but instead were regulated by other downstream processes. Given our collective results, we propose that *Xbp1* deficiency damages the adaptive capacity of the ER, which, after the commitment of progenitors to the eosinophil lineage, results in pronounced defects in the maturation of granule proteins and secretory-pathway function that feed back

to downregulate the expression of Gata1 and genes encoding eosinophil granule proteins in a futile attempt to allow survival of irremediable cellular stress.

DISCUSSION

In this study we have identified an unexpectedly selective requirement for the transcription factor XBP1 in eosinophil development. Through the use of multiple genetic and cellular models, we found that XBP1 was potently and selectively activated during eosinophil differentiation and was required in a cell-intrinsic way for the survival of committed EoPs. Loss of *Xbp1* resulted in the downregulation of a network of genes encoding products dedicated to preserving ER protein folding and homeostasis of secretory pathways in hematopoietic progenitors. After commitment of progenitors to the eosinophil lineage, those secretory-pathway vulnerabilities were overwhelmed, which resulted in critical defects in secretory granule formation, downregulation of expression of the gene encoding the major lineage determinant GATA-1 and loss of expression of genes encoding key eosinophil granule proteins. Collectively our data revealed that granulocytes could be distinguished by their reliance on maintaining homeostasis of the secretory pathway via the stress-response transcription factor XBP1.

Eosinophil development results from carefully coordinated activity of transcription factors such as GATA-1, PU.1, C/EBPα, C/EBPε and IRF8. Notably, all factors known to be involved in eosinophil development are also required by one or more alternative granulocyte lineages, which attests to the intimate transcriptional and ontological relatedness among neutrophils, basophils and eosinophils. We observed a complete loss of *Xbp1*^{Vav1} eosinophils starting at the EoP stage, with no effects on peripheral basophils or neutrophils, which established XBP1 as a factor exclusive for eosinophil development among granulocytes. The residual *Xbp1*^{Vav1} EoPs exhibited increased caspase activity relative to such activity in *Xbp1*$^{f/f}$ EoPs, which indicated that *Xbp1*^{Vav1} EoPs were eliminated by cell death. Furthermore, reduced eosinophil counts in *Xbp1*^{eoCRE} mice demonstrated that XBP1 operated after lineage commitment. As nascent granules are present in the earliest identifiable committed EoPs[19], these experiments traced the function of XBP1 to eosinophil granulogenesis.

We detected potent splicing of *Xbp1* mRNA in several myeloidprogenitor cell types along the eosinophil developmental continuum, which suggested that ER stress is a characteristic of steady-state hematopoiesis. This finding was consistent with published reports demonstrating that myelopoiesis is marked by increased protein synthesis and oxidative stress[35]. Unexpectedly, the phenotype of *Xbp1*^{Vav1} mice was exceedingly specific for eosinophils, which revealed that most cells did not require XBP1 to survive developmental stressors. XBP1 is required for immunoglobulin production by plasma cells, although *Xbp1*-deficient B220^{int}CD138^{+} intermediate forms of plasma cells are found in normal numbers *in vivo*[36]. Notably, we were unable to identify similar residual populations of immature eosinophils, which suggested that unlike plasma cells, committed eosinophils cannot exist in a partially mature state.

Eosinophils are singular among granulocytes in that they must safely store highly basic granule proteins (isoelectric point, >10) such as PRG2, EPX and the eosinophil-associated RNases, many of which are cytotoxic and/or exhibit membrane-destabilizing properties[37,38]. Additionally, eosinophils uniquely store certain granule proteins (PRG2) as crystalline depots[39,40] and are histologically identifiable by Congo red staining[41], suggestive of tightly regulated, physiological intracellular amyloid formation. Given these nuances of eosinophil granule development and function, it is notable that inefficient granule formation itself, although not excessive production of granule proteins, appears to be a major regulator of the survival of EoPs. Mice with heterozygous or homozygous deletion of various genes encoding products involved in pathways for the processing and disposal of secreted protein (such as *Galc*, *Atp6v0a1*, *Lyst* and *Txndc5*) are deficient in eosinophils[42]. Additionally, it has been demonstrated that eosinophil development crucially relies on production of the lineage-specific granule proteins PRG2 and EPX, which cumulatively occupy more than 50% of specific granules by volume[43]. That finding and the granule-formation defects observed in *Xbp1*^{Vav1} cells committed to the eosinophil lineage suggest that eosinophil development may require finely tuned expression of granule proteins, wherein too little or too much corrupts terminal differentiation. However, we found that wild-type BMDEs developed normally upon retroviral overexpression of PRG2 and/or EPX (data not shown), which suggested that eosinophil development is acutely sensitive to the scarcity and processing of granule proteins but can adapt to the excessive production of granule proteins.

Immunofluorescence analysis revealed that *Xbp1*^{Vav1} cells were able to produce eosinophil-specific granule proteins to a limited degree. Additionally, both PRG2 and EPX were consistently located within granule-like punctate structures in BMDEs (data not shown), which challenged the possibility of leakage of cytotoxic proteins due to granule destabilization. By driving GMPs into the eosinophil lineage via overexpression of GATA-2, we were able to detect severe blockades in the maturation of both EPX and PRG2, along with severe ultrastructural defects in granule nucleation. The lack of observable eosinophilic Wright-Giemsa staining in *Xbp1*^{Vav1} primary BMDEs confirmed the defect in eosinophil granule-protein maturation, as the acidic ‘pre-pro-’ portions block eosinophilic staining. The accumulation of these immature species correlated with transcriptional downregulation of genes encoding eosinophil granule proteins and the induction of ER stress–mediated PERK-ATF4 activity, in support of a model in which crucial components of the eosinophil developmental program are modulated on the basis of ER and granule ‘health’. It is possible that PERK, which is normally inactive during eosinophil differentiation, may mediate some of this feedback. Given the observed severity of the blockade, it is likely that *Xbp1*^{Vav1} cells never adequately resolved ER and granule stress, which resulted in sustained activation of PERK, permanent repression of the eosinophil developmental program and eventual cell death. Whether a complementary feedback loop exists to signal poor granule filling, as probably occurs in *Prg2*$^{-/-}$*Epx*$^{-/-}$ mice, remains to be determined.

We showed that both *Xbp1*^{Vav1} primary BMDEs and GATA-2-transduced *Xbp1*^{Vav1} GMPs substantially downregulated numerous genes encoding factors involved in the terminal differentiation of eosinophils, such as *Prg2* and *Epx*, relative to the expression of these

genes in their respective *Xbp1*$^{f/f}$ counterparts, yet these same genes were unaffected by short-term blockade of IRE1α-XBP1 signaling in BMDE cultures. Although spliced XBP1 protein itself has a relatively short half-life of just 22 min (ref. 1), the half-lives of the proteins encoded by its transcriptional target genes are considerably longer[44]. It is likely that persistent inhibition of XBP1-dependent signaling is needed to deplete the expression of target genes below the threshold necessary to maintain homeostasis of the ER and granules. Although the mechanism remains unclear, we have shown that this perturbation fed back to downregulate key elements of the eosinophil developmental program, including the gene encoding GATA-1, potentially as an adaptive mechanism to allow time for the disposal of accumulated misfolded proteins.

So far, XBP1 is the only transcription factor to our knowledge that distinguishes the development of eosinophils from that of other granulocytes, which suggests that subtle differences in cellular biological processes provide a previously unappreciated ‘handle’ for fine-tuning the production of different granulocyte subsets. Furthermore, our work has demonstrated that the function of XBP1 in cellular development could not be accurately predicted solely on the basis of the abundance of secreted protein production. Additional studies are needed to explore whether this selectivity derives from stress-mediated cell type–specific relationships between XBP1 and key developmental regulators such as GATA-1 or derives instead from particularly complex requirements for the folding of granule proteins. It is also possible that downregulation of the production of granule proteins is a common feature of granulocyte progenitors undergoing ER stress, but that eosinophils are selectively eliminated because the production of granule proteins itself is as important to survival as that of canonical lineage-determining factors[43]. Collectively, these results indicate that the IRE1α-XBP1 signaling pathway represents an additional pharmacologically tractable signaling axis for modulating eosinophil development with therapeutic potential for the treatment of a wide variety of eosinophil-mediated disorders.

METHODS

Materials

The IRE1α inhibitor 4μ8C was from Millipore. Antibody to (anti-) GATA-1 (D52H6), anti-β-actin (4967S) and anti-PERK (D11A8) were from Cell Signaling Technologies. J.J. Lee and N.A. Lee provided the rat monoclonal antibody to mouse PRG2 (MT-14.7) and the mouse monoclonal antibody to mouse EPX (MM25-82.2). Unless indicated otherwise, all antibodies for flow cytometry were from BioLegend. All cytokines were from Peprotech. Retroviral plasmids MSCV-GFP, MSCV-XBP1U/S-IRES-GFP, MSCV-XBP1S-IRES-GFP and MSCV-XBP1U-IRES-GFP have been described[45]. *Gata2* and *Prg2* were cloned into the plasmid MSCV-IRES-GFP by PCR with high-fidelity DNA polymerase (Kapa Biosystems) to generate MSCV-GATA-2-IRES-GFP and MSCV-PRG2-IRES-GFP. *Epx* was cloned by PCR into plasmid MSCV-IRES-hCD4 with high-fidelity DNA polymerase (Kapa Biosystems) to generate MSCV-EPX-IRES-hCD4.

Mice

Mice were housed in the specific pathogen–free facility of Weill Cornell Medical College and were handled in accordance with guidelines from the Research Animal Resource Center of the Center of Comparative Medicine and Pathology at Weill Cornell Medical College (protocol 2012-0004). Mice with hematopoietic system–specific or eosinophil-specific deletion of *Xbp1* were generated by mating of *Xbp1*$^{f/f}$ mice with the B6.Cg-Tg(*Vav1*-cre)A2Kio/J strain (Jackson Laboratory) or the eoCRE strain[23], respectively. *Ern1*$^{f/f}$ mice have been described[46] and were backcrossed with a 'speed congenic strategy' to a C57BL/6 background of greater than 98%, then were mated with *Vav1*-Cre mice to generate *Ern1*^{Vav1} mice. Congenic CD45.1^{+} C57BL/6 mice were from Jackson Laboratories. *Il5*-transgenic BALB/c mice were provided by C. Gerard. Sex- and age-matched littermates were used as controls throughout the study.

Cell culture

Bone marrow eosinophil cultures were prepared as described[25], with slight modification. Bone marrow cells were harvested from femurs, tibias and pelvic bones. After lysis of red blood cells, c-Kit^{+} hematopoietic&epsi progenitor cells were enriched by positive selection with anti-c-Kit MACS beads (Miltenyi Biotec) and were resuspended to a density of 1×10^6 cells per ml in RPMI-1640 medium (VWR) supplemented with 20% FBS (Atlanta Biologicals), 2 mM l-glutamine (Cellgro), 25 mM HEPES, pH 7.2–7.6 (Cellgro), non-essential amino acids (Cellgro), 1 mM sodium pyruvate, 100 U penicillin, 100 μg/ml streptomycin (Corning Cellgro), 50 μM β-mercaptoethanol (Sigma) and the cytokines SCF (100 ng/ml) and Flt3L (100 ng/ml), followed by culture for 4 d. After day 4, the cells were washed and then were cultured in the presence of IL-5 (10 ng/ml) for the duration of the culture, with medium changes on days 8 and 10. For certain experiments, BMDE cultures were supplemented with 10 ng/ml IL-3 and/or 10 ng/ml GM-CSF. Eosinophils from *Il5*-transgenic mice were isolated by mechanical disruption of the spleen as described[47]. For overnight incubation with the IRE1α inhibitor 4μ8C, bone marrow cells (after lysis of red blood cells) were cultured at a density of 1×10^6 cells per ml in complete RPMI medium supplemented with 10 ng/ml IL-5 to enhance eosinophil survival *in vitro*.

Sorted GMPs for retroviral transduction were cultured as described[31] with slight modification. Sorted cells were infected with retrovirus containing the plasmid MSCV-GATA-2-IRES-GFP and then were grown for 36 h in Iscove's modified Dulbecco's medium (Corning) containing 20% FBS, 100 U penicillin, 100 μg/ ml streptomycin and 50 μM β-mercaptoethanol supplemented with SCF (20 ng/ml), IL-3 (20 ng/ml), IL-5 (50 ng/lL), IL-6 (20 ng/ml), IL-7 (20 ng/ml), IL-11 (10 ng/ml) and GM-CSF (10 ng/ml). GFP^{+} cells were then re-sorted and then grown in SCF (20 ng/ml), IL-3 (20 ng/ml), IL-5 (50 ng/ml), and GM-CSF (10 ng/ml) for the remainder of the culture period (up to 5 d). Time in culture reported for all GATA-2-transduction experiments was measured starting after the second sort. Where indicated, cell morphology was assessed by cytospin followed by modified staining with Wright-Giemsa (WG16) according to the manufacturer's protocol (Sigma).

Retroviral infection

Retroviruses were produced by co-transfection of retroviral vectors with gag-pol and VSV-G expression plasmids into 293T cells through the use of Effectene reagent according to the manufacturer's instructions (Qiagen). Retroviral supernatants were harvested and then were concentrated 100× by ultracentrifugation for 2 h at 112,398*g* with a Sorvall SW-28 rotor. Concentrated viruses were used for 'spin-infection' of target primary cell cultures at 1,000*g* for 1.5 h at 32 °C in the presence of 8 μg/ml polybrene.

RNA extraction, RT-qPCR and XBP1 splicing assay

Total RNA was prepared with TRIzol according to the manufacturer's instructions (Invitrogen). cDNA was synthesized with a High Capacity cDNA Reverse Transcription Kit (Applied Biosystems). Quantitative RT-PCR was performed with SYBR Green fluorescent reagent on the Mx3005P QPCR System (Strategene). The amount of mRNA was normalized with *Actb* as a control by the comparative threshold cycle method. Efficiency of Cre recombinase– mediated deletion of *Xbp1* with loxP-flanked exon 2 was assessed by quantitative PCR as described[48]. Primer sequences used for quantitative PCR in this study are in Supplementary Table 4. The *Xbp1* mRNA–splicing assay was performed as described[21]. Primers surrounding the splice site in the *Xbp1* mRNA (5′-ACACGCTTGGGAATGGACAC-3′ and 5′-CCA TGGGAAGATGTTCTGGG-3′) were used for amplification by PCR, after which the products were separated by electrophoresis through a 2.5% agarose gel and visualized by staining with ethidium bromide. The frequency of *Xbp1* mRNA splicing was calculated by ImageJ software via densitometry as follows: intensity of *Xbp1s* band / ([intensity of *Xbp1s* band] + [intensity of *Xbp1us* band]) × 100.

Flow cytometry

Flow cytometry of bone marrow cells, splenocytes, blood cells and BMDEs was conducted using the following antibodies (all from BioLegend unless stated otherwise): anti-Gr-1 (RB6-8C5), anti-F4/80 (BM8), anti-Ly6G (1A8), anti-B220 (RA3-6B2), anti-CD11c (N418), anti-CD45.1 (A20), anti-CD45.2 (104), anti-Siglec-F (E50-2440; BD Pharmingen), anti-CCR3 (J073E5), anti-FcεRI (MAR-1), anti-CD4 (RM4-5), anti-CD8α (53-6.7), anti-CD16/32 (93), anti-CD11b (M1/70), antibody to IL-5 receptor-α (T21; BD Pharmingen), anti-CD34 (RAM34; eBioscience), anti-Ter119 (TER-119), anti-Sca-1 (D7), anti-CD3 (145-2C11) and anti-c-Kit (2B8). Events were acquired on an LSR II flow cytometer system (BD Biosciences) and data were analyzed with FlowJo software (TreeStar). Cell sorting was performed on a FACSAria II SORP cell sorter (Becton Dickinson) at Weill Cornell Medical College, with exclusion of $DAPI^+$ cells and doublets. Before sorting, stem and progenitor populations underwent initial enrichment by staining of cells with biotin-conjugated antibodies to lineage markers, followed by incubation with streptavidin MACS beads (Miltenyi Biotec) or by positive selection of $c\text{-}Kit^+$ cells with anti-c-Kit MACS beads (Miltenyi Biotec). Lineage markers used for GMP staining were defined as Gr-1, CD11c, CD11b, CD8α, CD4, CD3, B220 and Ter119, while lineage markers used for EoP staining were defined as Gr-1, CD11c, CD8α, CD4, CD3, B220 and Ter119. Caspase activity was measured with a CaspGLOW Fluorescein Active Caspase Staining Kit according to the

manufacturer's instructions (eBioscience). Staining with annexin V and propidium iodide for analysis of cell death was measured with an Annexin V Apoptosis Detection Kit APC according to the manufacturer's instructions (eBioscience).

Bone marrow chimeras

Recipient CD45.1$^+$ C57BL/6 mice were switched to a Sulfatrim diet 7 d before irradiation. Mice were then exposed to a single lethal full-body irradiation of 1,000 rads. 24 h after irradiation, 5×10^6 total bone marrow cells from a 1:1 mixture of wild-type C57BL/6 (CD45.1$^+$) bone marrow cells and *Xbp1*$^{f/f}$ or *Xbp1*^{Vav1} (CD45.2$^+$) bone marrow cells were injected into the irradiated hosts. The mice were maintained on a Sulfatrim diet for a minimum of 12 weeks, after which the proportion of engraftment from each donor was measured by flow cytometry.

Immunofluorescence

Suspension cells from BMDE cultures were transferred onto glass slides by cytospin and were fixed for 10 min at 25 °C with 4% paraformaldehyde. Cells were repeatedly washed with PBS, then nonspecific binding was blocked and cells were permeabilized by incubation for 30–60 min with 3% goat serum, 1% BSA and 0.1% Triton X-100 in PBS. Cells were then incubated overnight at 4 °C with anti-GATA-1 and anti-PRG2 (identified above) in PBS with 1% BSA and 0.1% Triton-X100. Primary antibodies were visualized by staining with secondary antibodies Alexa Fluor 555–conjugated goat anti-rat (A21434) and Alexa Fluor 488–conjugated goat anti-rabbit (A11029) (both from Molecular Probes), and cells were counterstained with 1 μg/ml DAPI (4,6-diamidino-2-phenylindole) and were mounted with Slowfade Gold (Life Technologies). Digital confocal images for quantification by ImageJ software were captured on an Olympus IX81. High-quality images were captured on an AxioVert LSM710 confocal microscope (Zeiss).

For image quantification, ImageJ software was used for determination of the average pixel intensity of 16-bit greyscale images from each channel individually. The fluorescence intensity of GATA-1 and PRG2 was calculated with ImageJ software as follows: corrected total cell fluorescence = region of interest integrated density – ([area of selected cell region of interest] × [mean fluorescence of background]).

Immunoblots

Cell pellets were lysed in RIPA buffer (50 mM Tris-HCl, pH 8.0, 150 mM NaCl, 1% NP40, 0.5% deoxycholate, 0.1% SDS and 50 mM NaF) supplemented with a protease inhibitor tablet. Homogenates were centrifuged at 12,000*g* for 10 min at 4 °C, and the supernatants were collected. Protein concentration in lysates was measured with a Pierce BCA Protein Assay Kit (Thermo Scientific) and equivalent amounts of protein were used for immunoblot analysis of GATA-1, PRG2, EPX and β-actin.

RNA-seq

Total RNA from GMPs and GATA-2-transduced GMPs was extracted with TRIzol according to the manufacturer's instructions. For GMPs, poly(A)$^+$ RNA-seq libraries were prepared with an Illumina TruSeq RNA Sample Preparation Kit V2 according to the

manufacturer's instructions (Illumina). For GATA-2-transduced GMPs, libraries for Illumina sequencing were obtained by the generation of double-stranded cDNA with a SMARTer UltraTMLow Input RNA Kit for Illumina sequencing (634826; Clontech Laboratories), followed by library preparation with a TruSeq sample preparation kit (IP-202-1012) according to the manufacturer's instructions (Illumina). Sequence data from Illumina's HiSeq2000 sequencer were 'de-multiplexed' to generate FASTQ files for each sample with Illumina's CASAVA pipeline (version 1.8.2).

The 'reads' that passed Illumina's quality and purity filter were aligned to the mouse genome (Illumina iGenomes mm9 build) with the STAR aligner program (version 2.3.0) with default parameters. The resulting SAM alignment files were then converted to the BAM file format, then were sorted and indexed with SAMtools (version 0.1.14). The HTSeq python package[49] was used for summarization of the aligned sequence reads into counts. Differential gene expression was analyzed with the DESeq Bioconductor package[50]. Transcripts were considered differentially expressed with a difference in expression of 1.5-fold or more and an adjusted *P* value (false-discovery rate) < 0.1. Pathway analysis of enriched gene ontology and predicted upstream transcriptional regulators was performed with Ingenuity Pathway Analysis software (Qiagen). For heat maps, variance-stabilized data from DESeq RNA-seq analyses were exported, manually curated for specific genes in each category, and the gene-expression z-score was visualized with the Heatmap.2 function within the gplots R library.

All differentially expressed transcripts identified by RNA-seq analyses of GATA-2-transduced GMPs were also compared with the 623 unique upregulated transcripts (*P* < 0.05; difference in expression of twofold or more) identified in a published study of BMDE maturation that examined IL-5-mediated transcriptional changes after 4 d in culture[31] (GEO accession code GSE55386).

Transmission electron microscopy

Cells were fixed with a modified Karmovsky's fix and a secondary fixation in reduced osmium tetroxide. Following dehydration, samples were embedded in an epon analog resin. Ultrathin sections (65 nm in thickness) were contrasted with lead citrate and were viewed on a JEM 1400 electron microscope (JEOL USA) operated at 120 kV. Digital images were captured on a Veleta 2K x 2K charge-coupled device camera (Olympus-SIS).

Statistical analyses

For comparison of two groups, data were analyzed by Student's *t*-test. When more than two groups were compared, data were analyzed by one-way or two-way ANOVA with the Šidák correction for multiple comparisons. All statistical analyses were performed with Graphpad Prism 6, with *P* values of <0.05 considered statistically significant.

Supplementary Material

Refer to Web version on PubMed Central for supplementary material.

Acknowledgments

We thank L. Cohen-Gould for assistance with electron microscopy; J. McCormick for assistance with cell sorting; the Starr Foundation Tri-Institutional Stem Cell Derivation Laboratory and Flow Cytometry and Microscopy Core facility for technical assistance, the Weill Cornell Epigenomics Core facility for library preparation and RNA sequencing; J. Cubillos-Ruiz and C. Tan for technical assistance; A. Espinosa, S. Hai and members of the Glimcher laboratory for suggestions and critical reading of this manuscript; A. Doyle for conversations; J.J. Lee and N.A. Lee (Mayo Clinic) for eoCRE mice, antibody to PRG2 and antibody to EPX; C. Gerard (Children's Hospital Medical, Boston) for *Il5*-transgenic BALB/c mice; and T. Iwawaki (Gunma University) for *Ern1*$^{f/f}$ mice. Supported by the US National Institutes of Health (R01DK082448 to L.H.G., R01HL095699 to L.A.S. and R37AI020241 to P.F.W.).

References

1. Calfon M, et al. IRE1 couples endoplasmic reticulum load to secretory capacity by processing the XBP-1 mRNA. Nature. 2002; 415:92–96. [PubMed: 11780124]
2. Harding HP, Zhang Y, Ron D. Protein translation and folding are coupled by an endoplasmic-reticulum-resident kinase. Nature. 1999; 397:271–274. [PubMed: 9930704]
3. Lu PD, Harding HP, Ron D. Translation reinitiation at alternative open reading frames regulates gene expression in an integrated stress response. J Cell Biol. 2004; 167:27–33. [PubMed: 15479734]
4. Lee AH, Iwakoshi NN, Glimcher LH. XBP-1 regulates a subset of endoplasmic reticulum resident chaperone genes in the unfolded protein response. Mol Cell Biol. 2003; 23:7448–7459. [PubMed: 14559994]
5. Shoulders MD, et al. Stress-independent activation of XBP1s and/or ATF6 reveals three functionally diverse ER proteostasis environments. Cell Rep. 2013; 3:1279–1292. [PubMed: 23583182]
6. Reimold AM, et al. Plasma cell differentiation requires the transcription factor XBP-1. Nature. 2001; 412:300–307. [PubMed: 11460154]
7. Kaser A, et al. XBP1 links ER stress to intestinal inflammation and confers genetic risk for human inflammatory bowel disease. Cell. 2008; 134:743–756. [PubMed: 18775308]
8. Lee AH, Chu GC, Iwakoshi NN, Glimcher LH. XBP-1 is required for biogenesis of cellular secretory machinery of exocrine glands. EMBO J. 2005; 24:4368–4380. [PubMed: 16362047]
9. Iwakoshi NN, Pypaert M, Glimcher LH. The transcription factor XBP-1 is essential for the development and survival of dendritic cells. J Exp Med. 2007; 204:2267–2275. [PubMed: 17875675]
10. Amulic B, Cazalet C, Hayes GL, Metzler KD, Zychlinsky A. Neutrophil function: from mechanisms to disease. Annu Rev Immunol. 2012; 30:459–489. [PubMed: 22224774]
11. Furuta GT, Atkins FD, Lee NA, Lee JJ. Changing roles of eosinophils in health and disease. Ann Allergy Asthma Immunol. 2014; 113:3–8. [PubMed: 24795292]
12. Karasuyama H, Mukai K, Obata K, Tsujimura Y, Wada T. Nonredundant roles of basophils in immunity. Annu Rev Immunol. 2011; 29:45–69. [PubMed: 21166539]
13. Wu D, et al. Eosinophils sustain adipose alternatively activated macrophages associated with glucose homeostasis. Science. 2011; 332:243–247. [PubMed: 21436399]
14. Qiu Y, et al. Eosinophils and type 2 cytokine signaling in macrophages orchestrate development of functional beige fat. Cell. 2014; 157:1292–1308. [PubMed: 24906148]
15. Heredia JE, et al. Type 2 innate signals stimulate fibro/adipogenic progenitors to facilitate muscle regeneration. Cell. 2013; 153:376–388. [PubMed: 23582327]
16. Simson L, et al. Regulation of carcinogenesis by IL-5 and CCL11: a potential role for eosinophils in tumor immune surveillance. J Immunol. 2007; 178:4222–4229. [PubMed: 17371978]
17. Chu VT, et al. Eosinophils are required for the maintenance of plasma cells in the bone marrow. Nat Immunol. 2011; 12:151–159. [PubMed: 21217761]
18. Bainton DF, Farquhar MG. Segregation and packaging of granule enzymes in eosinophilic leukocytes. J Cell Biol. 1970; 45:54–73. [PubMed: 5459000]

19. Iwasaki H, et al. Identification of eosinophil lineage-committed progenitors in the murine bone marrow. J Exp Med. 2005; 201:1891–1897. [PubMed: 15955840]
20. Voehringer D, van Rooijen N, Locksley RM. Eosinophils develop in distinct stages and are recruited to peripheral sites by alternatively activated macrophages. J Leukoc Biol. 2007; 81:1434–1444. [PubMed: 17339609]
21. Martinon F, Chen X, Lee AH, Glimcher LH. TLR activation of the transcription factor XBP1 regulates innate immune responses in macrophages. Nat Immunol. 2010; 11:411–418. [PubMed: 20351694]
22. Ma Y, Shimizu Y, Mann MJ, Jin Y, Hendershot LM. Plasma cell differentiation initiates a limited ER stress response by specifically suppressing the PERKdependent branch of the unfolded protein response. Cell Stress Chaperones. 2010; 15:281–293. [PubMed: 19898960]
23. Doyle AD, et al. Homologous recombination into the eosinophil peroxidase locus generates a strain of mice expressing Cre recombinase exclusively in eosinophils. J Leukoc Biol. 2013; 94:17–24. [PubMed: 23630390]
24. de Bruin AM, et al. Eosinophil differentiation in the bone marrow is inhibited by T cell-derived IFN-γ. Blood. 2010; 116:2559–2569. [PubMed: 20587787]
25. Dyer KD, et al. Functionally competent eosinophils differentiated ex vivo in high purity from normal mouse bone marrow. J Immunol. 2008; 181:4004–4009. [PubMed: 18768855]
26. Cross BC, et al. The molecular basis for selective inhibition of unconventional mRNA splicing by an IRE1-binding small molecule. Proc Natl Acad Sci USA. 2012; 109:E869–E878. [PubMed: 22315414]
27. Tominaga A, et al. Transgenic mice expressing a B cell growth and differentiation factor gene (interleukin 5) develop eosinophilia and autoantibody production. J Exp Med. 1991; 173:429–437. [PubMed: 1988543]
28. Acosta-Alvear D, et al. XBP1 controls diverse cell type- and condition-specific transcriptional regulatory networks. Mol Cell. 2007; 27:53–66. [PubMed: 17612490]
29. Uhm TG, Kim BS, Chung IY. Eosinophil development, regulation of eosinophilspecific genes, and role of eosinophils in the pathogenesis of asthma. Allergy Asthma Immunol Res. 2012; 4:68–79. [PubMed: 22379601]
30. Satoh T, et al. Critical role of Trib1 in differentiation of tissue-resident M2-like macrophages. Nature. 2013; 495:524–528. [PubMed: 23515163]
31. Iwasaki H, et al. The order of expression of transcription factors directs hierarchical specification of hematopoietic lineages. Genes Dev. 2006; 20:3010–3021. [PubMed: 17079688]
32. Fulkerson PC, Schollaert KL, Bouffi C, Rothenberg ME. IL-5 triggers a cooperative cytokine network that promotes eosinophil precursor maturation. J Immunol. 2014; 193:4043–4052. [PubMed: 25230753]
33. Han J, et al. ER-stress-induced transcriptional regulation increases protein synthesis leading to cell death. Nat Cell Biol. 2013; 15:481–490. [PubMed: 23624402]
34. Fujiwara T, et al. Discovering hematopoietic mechanisms through genome-wide analysis of GATA factor chromatin occupancy. Mol Cell. 2009; 36:667–681. [PubMed: 19941826]
35. Tothova Z, et al. FoxOs are critical mediators of hematopoietic stem cell resistance to physiologic oxidative stress. Cell. 2007; 128:325–339. [PubMed: 17254970]
36. Todd DJ, et al. XBP1 governs late events in plasma cell differentiation and is not required for antigen-specific memory B cell development. J Exp Med. 2009; 206:2151–2159. [PubMed: 19752183]
37. Acharya KR, Ackerman SJ. Eosinophil granule proteins: form and function. J Biol Chem. 2014; 289:17406–17415. [PubMed: 24802755]
38. Kroegel C, Costabel U, Matthys H. Mechanism of membrane damage mediated by eosinophil major basic protein. Lancet. 1987; 1:1380–1381. [PubMed: 2884488]
39. Barker RL, Gleich GJ, Pease LR. Acidic precursor revealed in human eosinophil granule major basic protein cDNA. J Exp Med. 1988; 168:1493–1498. [PubMed: 3171483]
40. Soragni A, et al. Toxicity of eosinophil MBP is repressed by intracellular crystallization and promoted by extracellular aggregation. Mol Cell. 2015; 57:1011–1021. [PubMed: 25728769]

41. Grouls V, Helpap B. Selective staining of eosinophils and their immature precursors in tissue sections and autoradiographs with Congo red. Stain Technol. 1981; 56:323–325. [PubMed: 6171062]

42. Brown SD, Moore MW. The International Mouse Phenotyping Consortium: past and future perspectives on mouse phenotyping. Mammalian Genome. 2012; 23:632–640. [PubMed: 22940749]

43. Doyle AD, et al. Expression of the secondary granule proteins major basic protein 1 (MBP-1) and eosinophil peroxidase (EPX) is required for eosinophilopoiesis in mice. Blood. 2013; 122:781–790. [PubMed: 23736699]

44. Schwanhäusser B, et al. Global quantification of mammalian gene expression control. Nature. 2011; 473:337–342. [PubMed: 21593866]

46. Wang HB, Ghiran I, Matthaei K, Weller PF. Airway eosinophils: allergic inflammation recruited professional antigen-presenting cells. Journal of immunology. 2007; 179(11):7585–7592.

47. Jurczak MJ, Lee AH, Jornayvaz FR, Lee HY, Birkenfeld AL, Guigni BA, et al. Dissociation of inositol-requiring enzyme (IRE1alpha)-mediated c-Jun N-terminal kinase activation from hepatic insulin resistance in conditional X-box-binding protein-1 (XBP1) knock-out mice. The Journal of biological chemistry. 2012; 287(4):2558–2567. [PubMed: 22128176]

48. Anders S, Pyl PT, Huber W. HTSeq-a Python framework to work with high-throughput sequencing data. Bioinformatics. 2015; 31(2):166–169. [PubMed: 25260700]

49. Anders S, Huber W. Differential expression analysis for sequence count data. Genome biology. 2010; 11(10):R106. [PubMed: 20979621]

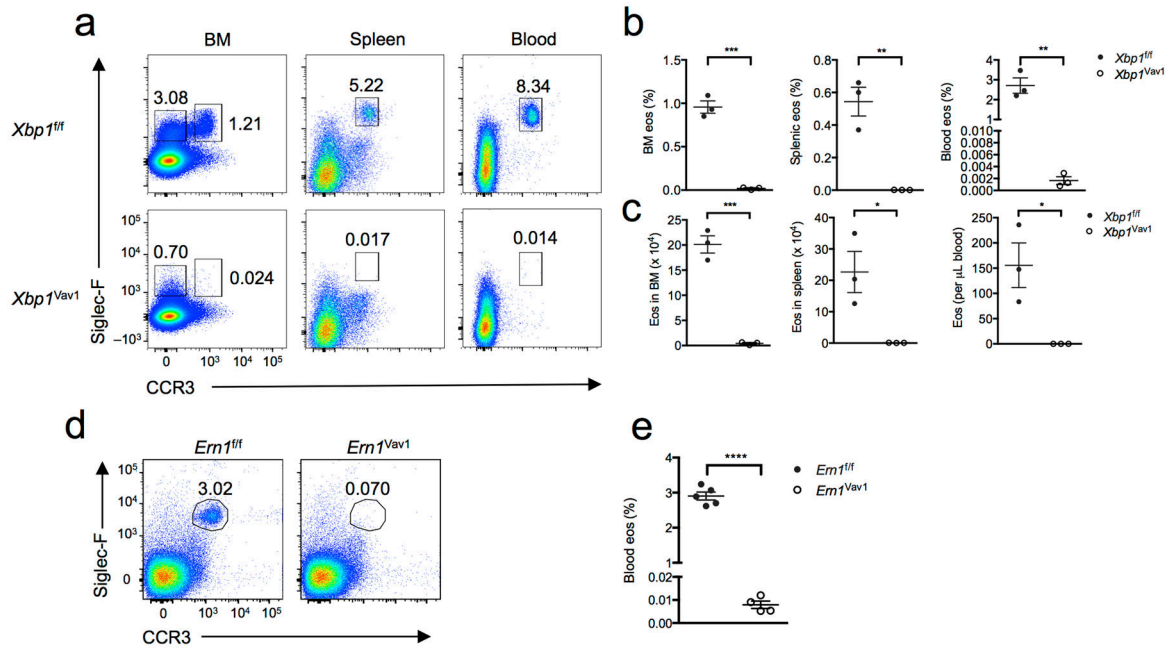

Figure 1.

XBP1 is required for eosinophil differentiation. (**a**) Flow cytometry of cells from the bone marrow (BM), spleen and blood of *Xbp1*$^{f/f}$ and *Xbp1*^{Vav1} mice, gated on non-B, non-T cells (spleen and blood only). Numbers adjacent to outlined areas indicate percent Siglec-F^{+}CCR3^{+} mature eosinophils (top right) or Siglec-F^{+}CCR3^{-} immature bone marrow eosinophils (top left, far left column). (**b**) Frequency of mature (Siglec-F^{+}CCR3^{+}) eosinophils (eos) in the bone marrow, spleen and blood of *Xbp1*$^{f/f}$ and *Xbp1*^{Vav1} mice (n = 3 per genotype). (**c**) Absolute number of mature eosinophils in the bone marrow (two tibias and two femurs per mouse), spleen and blood of *Xbp1*$^{f/f}$ and *Xbp1*^{Vav1} mice (n = 3 per genotype). (**d**) Flow cytometry of cells from the blood of Ern1$^{f/f}$ and Ern1^{Vav1} mice. Numbers adjacent to outlined areas indicate percent Siglec-F^{+}CCR3^{+} mature eosinophils. (**e**) Frequency of mature eosinophils in blood of *Ern1*$^{f/f}$ mice (n = 5) and *Ern1*^{Vav1} mice (n = 4). Each symbol (**b**,**c**,**e**) represents an individual mouse; small horizontal lines indicate the mean (± s.e.m.). *P < 0.05, **P < 0.01, ***P < 0.001 and ****P < 0.0001 (Student's t-test). Data are representative of at least three independent experiments with at least three mice per group in each.

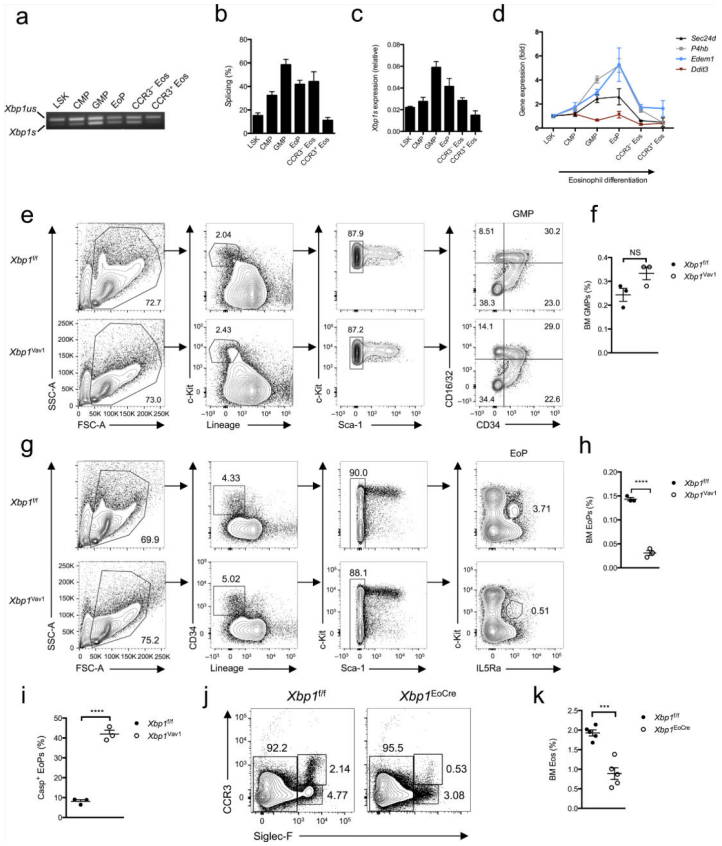

Figure 2.

XBP1 is potently activated during eosinophil differentiation *in vivo* and is required upon commitment to the eosinophil lineage. (**a**) PCR analysis of spliced (*Xbp1s*) and unspliced (*Xbp1us*) *Xbp1* mRNA in LSK cells, CMPs, GMPs, EoPs and CCR3^{-} or CCR3^{+} eosinophils purified by flow cytometry. (**b**) Frequency of *Xbp1s* mRNA among total *Xbp1* mRNA in sorted LSK cells, CMPs, GMPs, EoPs, CCR3^{-} eosinophils, and CCR3^{+} eosinophils (n = 3 mice per cell type). (**c**) Quantitative PCR analysis of the *Xbp1s* isoform in cells as in a (n = 3 mice per cell type); results were normalized to those of *Actb*. (**d**) Quantitative PCR analysis of *Sec24d*, *P4hb*, *Edem1* and *Ddit3* in cells as in a (n = 3 mice per cell type); results (normalized as in **c**) are presented relative to those of LSK cells. (**e**) Gating strategy for flow cytometry of bone marrow GMPs from *Xbp1*$^{f/f}$ and *Xbp1*^{Vav1} mice. Numbers adjacent to outlined areas indicate percent cells with leukocyte side scatter (SSC-A) or forward scatter (FSC-A) (far left), c-Kit^{+}Lin^{-} cells (middle left) or c-Kit^{+}Sca-1^{-} cells (middle right); numbers in quadrants indicate percent GMPs in each (far right). (**f**) Frequency of GMPs in the bone marrow of *Xbp1*$^{f/f}$ and *Xbp1*^{Vav1} mice (n = 3 per genotype). (**g**) Gating strategy for flow cytometry of bone marrow EoPs from *Xbp1*$^{f/f}$ and *Xbp1*^{Vav1} mice. Numbers adjacent to outlined areas indicate percent cells with leukocyte side or forward scatter (far left), CD34^{+}Lin^{-} cells (middle left), c-Kitpos–negSca-1^{-} cells (middle right) or c-KitintIL-5Rα^{+} cells (far right). (**h**) Frequency of EoPs in bone marrow from *Xbp1*$^{f/f}$ and *Xbp1*^{Vav1} mice (n = 3 per genotype). (**i**) Frequency of EoPs exhibiting caspase activity (Casp^{+}), assessed by flow cytometry (n = 3 mice per genotype). (**j**) Flow cytometry of eosinophils in bone marrow from *Xbp1*$^{f/f}$ and *Xbp1*^{eoCRE} mice. Numbers adjacent to outlined areas indicate

percent CCR3pos–negSiglec-F^{-} cells (left), CCR3^{+}Siglec-F^{+} cells (top right) or CCR3^{-}Siglec-F^{+} cells (bottom right). (**k**) Frequency of eosinophils in bone marrow from *Xbp1*$^{f/f}$ and *Xbp1*^{eoCRE} mice (n = 5 mice per genotype). Each symbol (**f**,**h**,**i**,**k**) represents an individual mouse; small horizontal lines indicate the mean (± s.e.m.). NS, not significant ($P > 0.05$); *$P < 0.001$ and **$P < 0.0001$ (Student's *t*-test). Data are from one experiment representative of three experiments with more than three independent biological replicates (**a**) or are representative of at least three independent experiments with at least three mice per group in each (**b**–**k**; mean and s.e.m. in **b**–**d**,**f**,**h**,**i**,**k**).

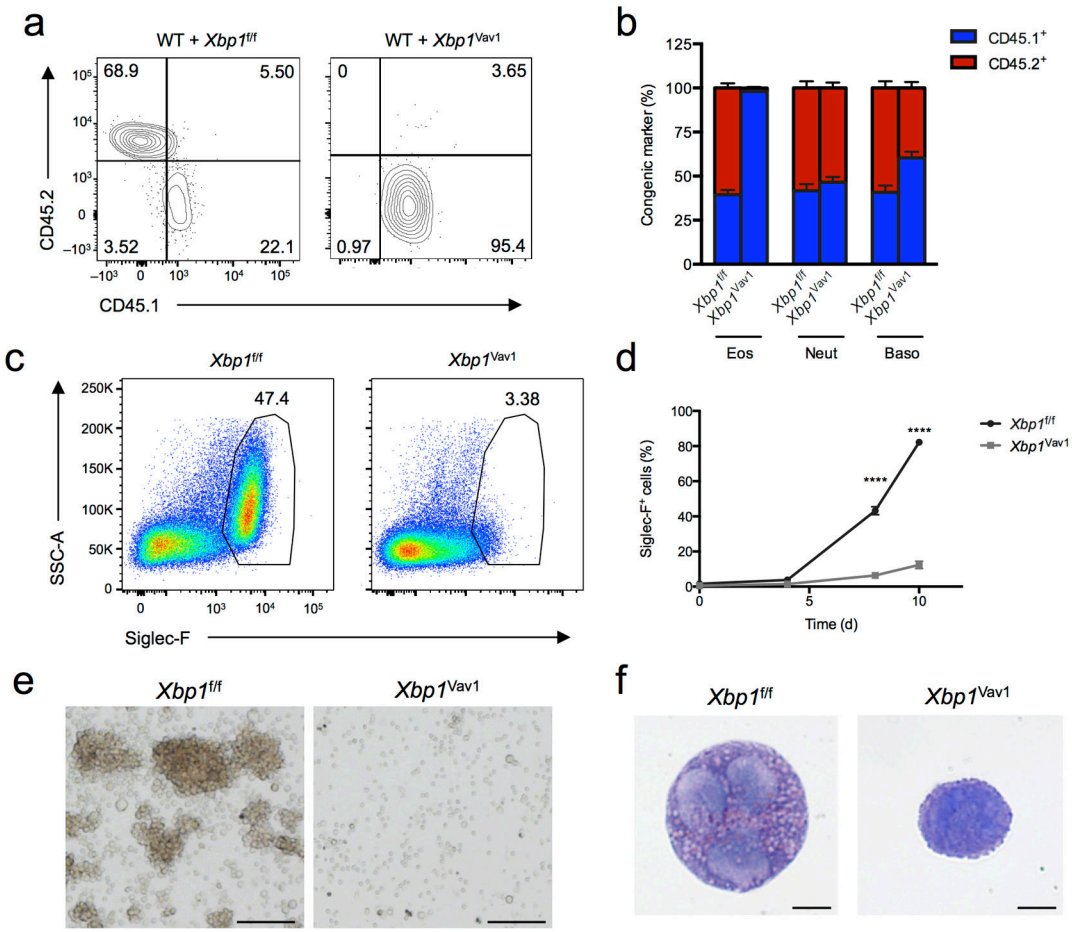

Figure 3.

XBP1 is a cell-intrinsic requirement for eosinophil development. (**a**) Flow cytometry assessing expression of the congenic markers CD45.2 (*Xbp1*$^{f/f}$ or *Xbp1*^{Vav1}) and CD45.1 (wild type) on peripheral blood eosinophils from chimeras generated with a mixture of wild-type bone marrow plus either *Xbp1*$^{f/f}$ bone marrow (WT $^{+}$ *Xbp1*$^{f/f}$) or *Xbp1*^{Vav1} bone marrow (WT $^{+}$ *Xbp1*^{Vav1}). Numbers in quadrants indicate percent cells in each. (**b**) Reconstitution efficiency of eosinophils, neutrophils (Neut) and basophils (Baso) in blood from mixed-bone marrow chimeras as in **a** (n = 6 host mice per chimera type). (**c**) Flow cytometry analyzing Siglec-F expression *Xbp1*$^{f/f}$ and *Xbp1*^{Vav1} BMDEs at day 8 of culture, gated on DAPI^{-} singlets. Numbers adjacent to outlined areas indicate percent Siglec-F^{+} cells. (**d**) Frequency of Siglec-F^{+} cells among *Xbp1*$^{f/f}$ and *Xbp1*^{Vav1} BMDEs at days 0, 4, 8 and 10 of culture (n = 3 independent cultures per genotype). (**e**) Microscopy of hematopoietic colonies from *Xbp1*$^{f/f}$ and *Xbp1*^{Vav1} BMDEs at day 8 of culture. Scale bars, 100 μm. (**f**) Microscopy of cytospin analysis of DAPI^{-}Siglec-F^{+} singlets sorted from *Xbp1*$^{f/f}$ and *Xbp1*^{Vav1} BMDEs at day 8 of culture. Scale bars, 5 μm. *P < 0.0001 (two-way analysis of variance (ANOVA) with the Šidák correction for multiple comparisons). Data are from two independent experiments with six mice per group (**a**,**b**; mean and s.e.m. in **b**) or more than three independent experiments with at least three mice per group (**c–f**; mean and s.e.m. in **d**).

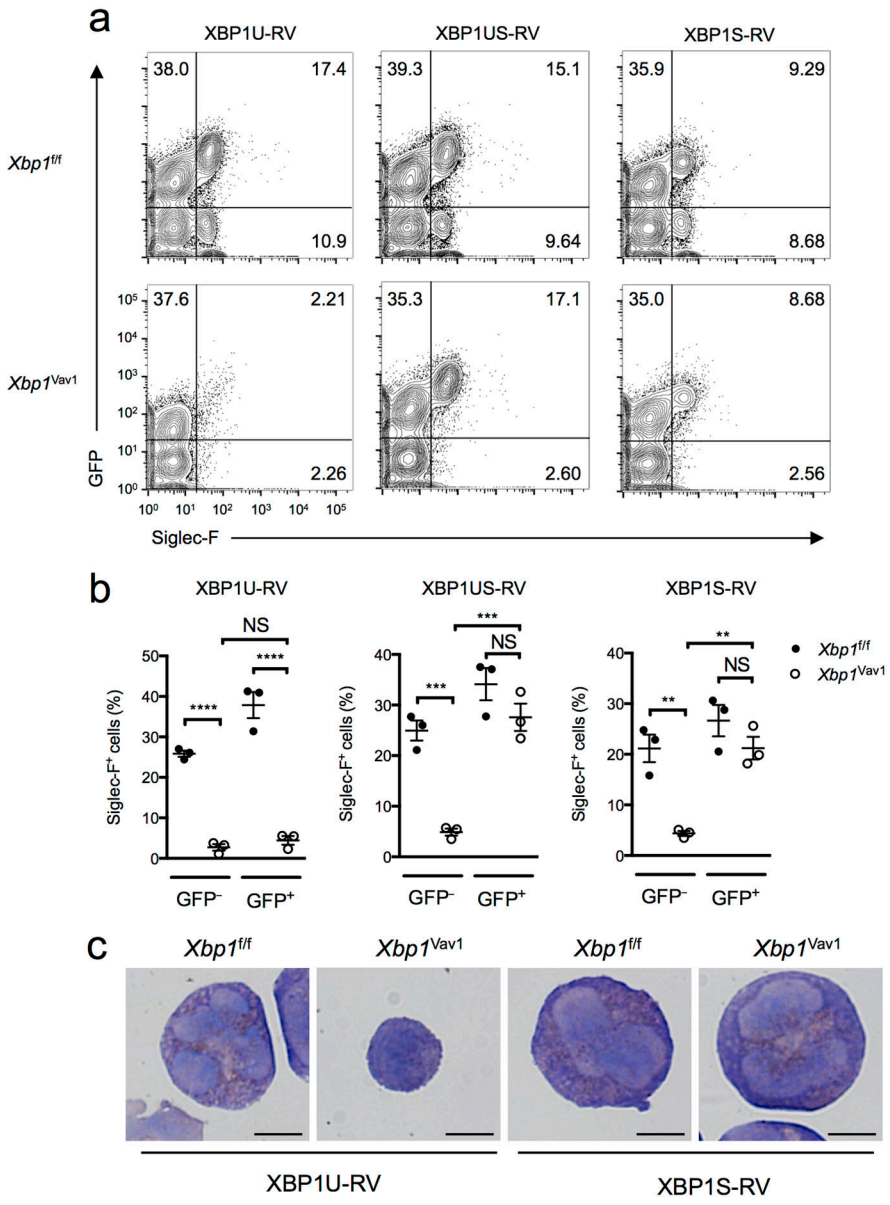

Figure 4.

Xbp1s can restore eosinophil development in *Xbp1*-deficient bone marrow cultures, but *Xbp1u* cannot. (**a**) Flow cytometry analyzing the expression of GFP and Siglec-F in *Xbp1*$^{f/f}$ and *Xbp1*^{Vav1} BMDEs transduced with retrovirus expressing *Xbp1u* mRNA (XBP1U-RV), *Xbp1us* mRNA (XBP1US-RV) or *Xbp1s* mRNA (XBP1S-RV) assessed at day 8 of culture. Numbers in quadrants indicate percent cells in each. (**b**) Frequency of Siglec-F^{+} eosinophils among total GFP^{-} and GFP^{+} cells from *Xbp1*$^{f/f}$ and *Xbp1*^{Vav1} BMDE cultures transduced as in a. Each symbol represents an individual mouse (n = 3 per genotype); small horizontal lines indicate the mean (± s.e.m.). (**c**) Microscopy of cytospin analyses of GFP^{+}Siglec-F^{+} cells sorted from *Xbp1*$^{f/f}$ and *Xbp1*^{Vav1} BMDEs transduced as in a (below images), assessed at day 8 of culture. Scale bars, 5 μm. *P < 0.01, **P < 0.001 and ***P < 0.0001 (one-way

ANOVA with the Holm-Šidák correction for multiple comparisons). Data are representative of three independent experiments with three biological replicates in each.

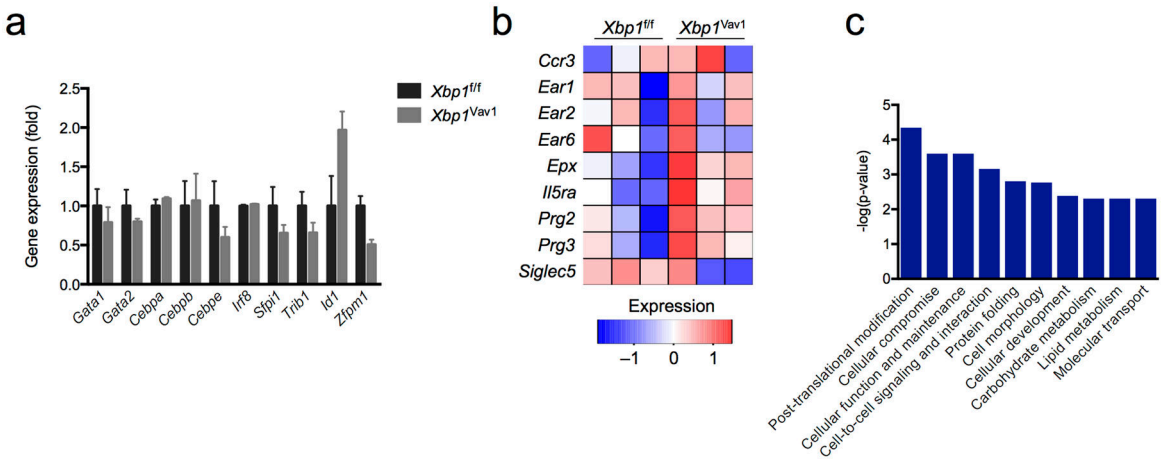

Figure 5.

The GMP-differentiation capacity is not affected by *Xbp1* deficiency. (**a**) Quantitative PCR analysis of genes encoding products known to regulate eosinophil differentiation, in sorted GMPs from *Xbp1*$^{f/f}$ and *Xbp1*^{Vav1} mice (n = 3 per genotype); results were normalized to those of *Actb* and are presented relative to those of *Xbp1*$^{f/f}$ GMPs. (**b**) RNA-seq analysis of selected genes encoding eosinophil markers, in *Xbp1*$^{f/f}$ and *Xbp1*^{Vav1} GMPs (n = 3 mice per genotype). (**c**) Pathway analysis of the ten molecular and cellular gene-ontology functions most significantly dysregulated in *Xbp1*^{Vav1} GMPs relative to their regulation in *Xbp1*$^{f/f}$ GMPs, ranked by *P* value from most significant (left) to least significant (right); results are presented as raw *P* values. Data are representative of three independent experiments (**a**; mean and s.e.m.) or one experiment with three independent biological replicates per group (**b**,**c**).

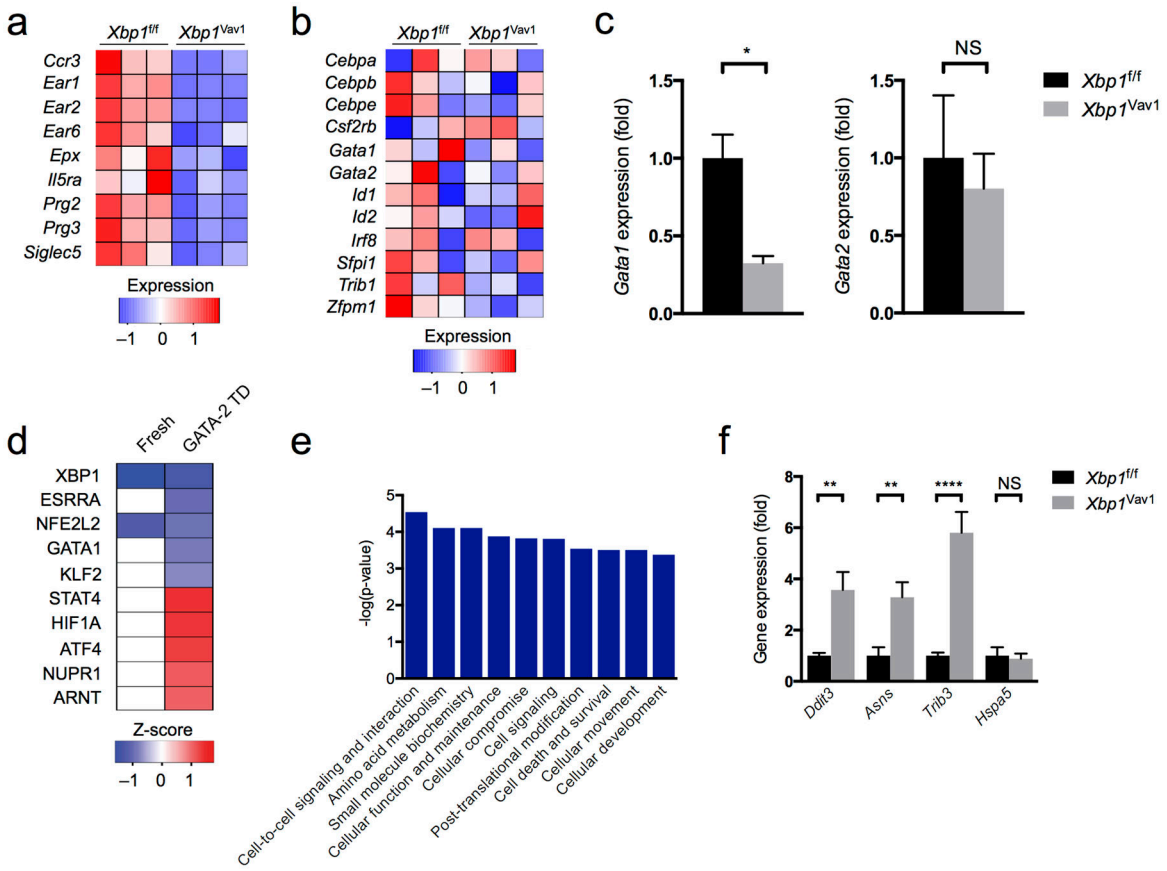

Figure 6.

Loss of XBP1-mediated protein-quality-control mechanisms interferes with eosinophil transcriptional identity. (**a**,**b**) RNA-seq analysis of genes encoding eosinophil markers (**a**) or regulators of eosinophil development (**b**), in GATA-2-transduced *Xbp1*$^{f/f}$ and *Xbp1*^{Vav1} GMPs (n = 3 independent cultures per genotype). (**c**) Quantitative PCR analysis of *Gata1* and *Gata2* in GATA-2-transduced *Xbp1*$^{f/f}$ and *Xbp1*^{Vav1} GMPs (n = 3 independent cultures per genotype) (presented as in Fig. 5a). (**d**) Pathway analysis–predicted top five activated or inhibited upstream transcriptional regulators (ranked by activation z-score) most responsible for the transcriptional differences between GATA-2-transduced (GATA-2 TD) *Xbp1*$^{f/f}$ GMPs and GATA-2-transduced *Xbp1*^{Vav1} GMPs, showing functional repression (blue) or activation (red) in *Xbp1*^{Vav1} cells compared with *Xbp1*$^{f/f}$ cells, and predicted influence on freshly sorted GMPs (Fresh). (**e**) Pathway analysis–predicted ten most significantly dysregulated molecular and cellular gene-ontology functions in GATA-2-transduced *Xbp1*$^{f/f}$ and *Xbp1*^{Vav1} GMPs (presented as in Fig. 5b). (**f**) Quantitative PCR analysis of *Ddit3*, *Asns*, *Trib3* and *Hspa5* in GATA-2-transduced *Xbp1*$^{f/f}$ and *Xbp1*^{Vav1} GMPs (n = 3 independent cultures per genotype) (presented as in Fig. 5a). **P* < 0.05, ***P* < 0.01 and ****P* < 0.0001 (Student's *t*-test (**c**) or one-way ANOVA with the Holm-Šidák correction for multiple comparisons (**f**)). Data are representative of one experiment (**a**,**b**,**d**,**e**) or two independent experiments with three independent biological replicates per group (**c**,**f**; mean and s.e.m.).

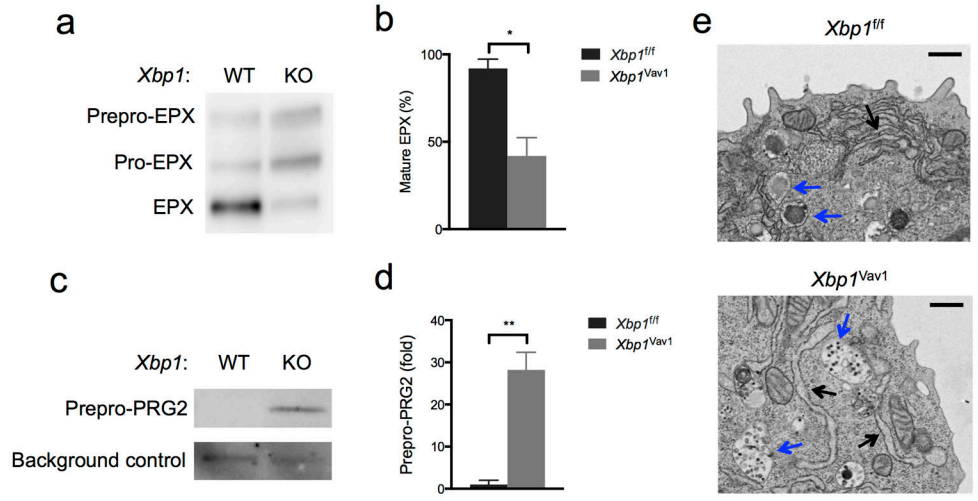

Figure 7.

Xbp1 deficiency causes defects in granule-protein maturation and secretory-pathway ultrastructure. (**a**) Immunoblot analysis of EPX maturation (left margin) in GATA-2-transduced *Xbp1*$^{f/f}$ (f/f) and *Xbp1*^{Vav1} (Vav1) GMPs. (**b**) Frequency of mature EPX in GATA-2-transduced *Xbp1*$^{f/f}$ and *Xbp1*^{Vav1} GMPs (n = 3 independent cultures per genotype). (**c**) Immunoblot analysis of the maturation of pre-pro-PRG2 in GATA-2-transduced *Xbp1*$^{f/f}$ and *Xbp1*^{Vav1} GMPs; below (Ctrl), nonspecific background band (loading control). (**d**) Abundance of immature pro-PRG2 (pre-pro-PRG2) in GATA-2-transduced *Xbp1*$^{f/f}$ and *Xbp1*^{Vav1} GMPs (n = 3 independent cultures per genotype); results were normalized to those of the nonspecific background band and are presented relative those of *Xbp1*$^{f/f}$ GMPs. (**e**) Transmission electron microscopy of GATA-2-transduced *Xbp1*$^{f/f}$ and *Xbp1*^{Vav1} GMPs: blue arrows indicate developing secretory granules; black arrows indicate the ER. Scale bars, 500 nm. *$P < 0.05$ and **$P < 0.01$ (Student's *t*-test). Data are representative of (**a**,**c**,**e**) or from (**b**,**d**) one experiment with three independent biological replicates per group (mean and s.e.m. in **b**,**d**).

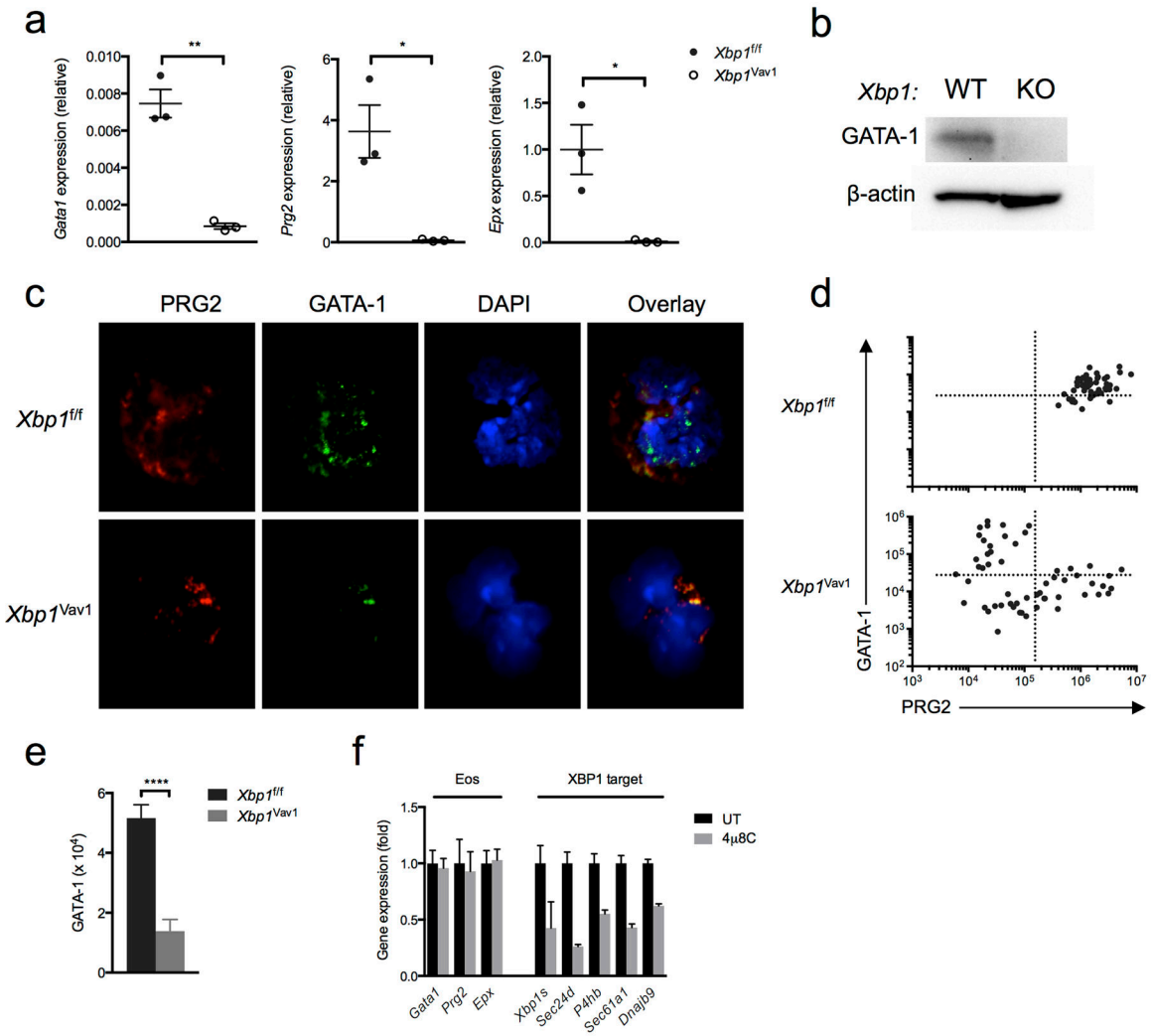

Figure 8.

Xbp1 deficiency prevents the accumulation of GATA-1 in eosinophils through an indirect mechanism. (**a**) Quantitative PCR analysis of *Gata1*, *Prg2* and *Epx* in sorted DAPI^{-}Siglec-F^{+} BMDEs from *Xbp1*$^{f/f}$ and *Xbp1*^{Vav1} mice (n = 3 independent cultures per genotype), assessed at day 8 of culture; results were normalized to those of *Actb*. (**b**) Immunoblot analysis of GATA-1 and β-actin (loading control) in *Xbp1*$^{f/f}$ and *Xbp1*^{Vav1} BMDEs at day 8 of culture. (**c**) Immunofluorescence microscopy of developing eosinophils among *Xbp1*$^{f/f}$ and *Xbp1*^{Vav1} BMDEs at day 8 of culture, stained for PRG2, GATA-1 and DAPI. (**d**) Scatter plots of PRG2 fluorescence versus GATA-1 fluorescence in *Xbp1*$^{f/f}$ BMDEs (n = 50) and *Xbp1*^{Vav1} BMDEs (n = 56) at day 8 of culture. (**e**) Staining intensity of GATA-1 in developing PRG2^{+} eosinophils among *Xbp1*$^{f/f}$ BMDEs (n = 47) and *Xbp1*^{Vav1} BMDEs (n = 30) at day 8 of culture. (**f**) Quantitative PCR analysis of the canonical eosinophil genes *Gata1*, *Prg2* and *Epx*, as well as *Xbp1s* and the *XBP1* target genes *Sec24d*, *P4hb*, *Sec61a1* and *Dnajb9*, in BMDE cultures treated for 8 h with the vehicle dimethyl sulfoxide (DMSO) or 4μ8C (20 μM) (n = 3 independent cultures per condition); results were normalized to those of *Actb* and are presented relative to those of vehicle-treated cells. *P < 0.05 and **P

< 0.01 and ***P < 0.0001 (Student's t-test). Data are representative of at least two independent experiments (**a**,**f**; mean and s.e.m.), two independent experiments (**b**) or two experiments with three independent biological replicates per genotype (**c**) or are from one experiment with three biological replicates pooled per genotype (**d**,**e**; mean and s.e.m. in **e**).